Global Change Biology

Global Change Biology (2016) **22**, 727–740, doi: 10.1111/gcb.13075

Past and future evolution of *Abies alba* forests in Europe – comparison of a dynamic vegetation model with palaeo data and observations

MELANIE RUOSCH[1,2], RENATO SPAHNI[1,2], FORTUNAT JOOS[1,2], PAUL D. HENNE[1,3], WILLEM O. VAN DER KNAAP[1,3] and WILLY TINNER[1,3]

[1]*Oeschger Centre for Climate Change Research, University of Bern, Falkenplatz 16, 3012 Bern, Switzerland,* [2]*Climate and Environmental Physics, Physics Institute, University of Bern, Sidlerstrasse 5, 3012 Bern, Switzerland,* [3]*Palaeoecology, Institute of Plant Sciences, University of Bern, Altenbergrain 21, 3013 Bern, Switzerland*

Abstract

Information on how species distributions and ecosystem services are impacted by anthropogenic climate change is important for adaptation planning. Palaeo data suggest that *Abies alba* formed forests under significantly warmer-than-present conditions in Europe and might be a native substitute for widespread drought-sensitive temperate and boreal tree species such as beech (*Fagus sylvatica*) and spruce (*Picea abies*) under future global warming conditions. Here, we combine pollen and macrofossil data, modern observations, and results from transient simulations with the LPX-Bern dynamic global vegetation model to assess past and future distributions of *A. alba* in Europe. LPX-Bern is forced with climate anomalies from a run over the past 21 000 years with the Community Earth System Model, modern climatology, and with 21st-century multimodel ensemble results for the high-emission RCP8.5 and the stringent mitigation RCP2.6 pathway. The simulated distribution for present climate encompasses the modern range of *A. alba*, with the model exceeding the present distribution in north-western and southern Europe. Mid-Holocene pollen data and model results agree for southern Europe, suggesting that at present, human impacts suppress the distribution in southern Europe. Pollen and model results both show range expansion starting during the Bølling–Allerød warm period, interrupted by the Younger Dryas cold, and resuming during the Holocene. The distribution of *A. alba* expands to the north-east in all future scenarios, whereas the potential (currently unrealized) range would be substantially reduced in southern Europe under RCP8.5. *A. alba* maintains its current range in central Europe despite competition by other thermophilous tree species. Our combined palaeoecological and model evidence suggest that *A. alba* may ensure important ecosystem services including stand and slope stability, infrastructure protection, and carbon sequestration under significantly warmer-than-present conditions in central Europe.

Keywords: *Abies alba*, climate projections, deglaciation, dynamic global vegetation model, global warming, Holocene, pollen data, vegetation dynamics

Received 7 May 2015; revised version received 6 August 2015 and accepted 7 August 2015

Introduction

The abundances and ranges of European plant species are projected to shift over the 21st century and beyond due to rapid and large climatic changes (Thuiller *et al.*, 2005; Meier *et al.*, 2012; IPCC, 2014). Although the anticipated invasions, range expansions, contractions, and extinctions of species have important implications for ecosystem services, such projections are affected by uncertainties (Schröter *et al.*, 2005; Cheaib *et al.*, 2012). In particular, modelling approaches that infer bioclimatic relationships from present species distributions can underestimate future potential when species ranges are constrained by nonclimatic factors such as human disturbance (García-Valdés *et al.*, 2013). Palaeoecological data that document past species distributions and process-based models that use plant physiological traits can both help address such uncertainties. Abundances and ranges of European plant species shifted repeatedly and dramatically in response to past climate change (Overpeck *et al.*, 2003; IPCC, 2014). Thus, palaeoecological data reveal the sensitivity of ecosystems and species to a broad range of environmental conditions and are needed to understand potential plant distributions under present and future climate. Dynamic global vegetation models (DGVM) are important tools for analysing and estimating the possible extent and impacts of future climate change on vegetation at continental scales (Joos *et al.*, 2001; Gerber *et al.*, 2004; Hickler *et al.*, 2012; Poulter *et al.*, 2013). Combining such process-based models with palaeoecology

Correspondence: Fortunat Joos, tel. +41 31 631 44 61, fax +41 31 631 87 42, e-mail: joos@climate.unibe.ch

contributes to a better understanding of species potential under global warming conditions, given that palaeoecological records may be used to validate model projections of species dynamics in response to climatic change (Anderson *et al*., 2006; Schwörer *et al*., 2014; Henne *et al*., 2015).

Palaeoecological records from the Italian Peninsula suggest that *Abies alba* (silver fir), a European tree species of paramount ecological and economic relevance, formed forests under significantly warmer-than-present conditions during the mid-Holocene and the Eemian (Tinner *et al*., 2013; Di Pasquale *et al*., 2014; Cunill *et al*., 2015). This finding contrasts with recent modelling efforts that concluded the range of *A. alba* may decline in Europe in response to global warming (Maiorano *et al*., 2013; Cailleret *et al*., 2014). The discrepancy between the assessments mainly derives from differing assumptions about the environmental constraints on *A. alba* populations in southern Europe. Approaches that assume distributions are in equilibrium with climate may underestimate *A. alba* potential in warm climates if millennia of land use eliminated *A. alba* from the warmest portions of its potential range. Some of the former habitats of *A. alba* are currently occupied by widespread European tree species such as *Fagus sylvatica* (beech) and *Picea abies* (spruce), which have been favoured by humans [e.g. (Küster, 1997; Markgraf, 1970; Ralska-Jasiewiczowa *et al*., 2003; Schwörer *et al*., 2015)], but are more drought-sensitive than *A. alba* (Ellenberg, 2009; Ellenberg & Leuschner, 2010; Henne *et al*., 2011). Given its past ecology, it has been suggested that under future climate warming and moderate human disturbance, *A. alba* might have the potential to replace these species and to thus ensure provisioning services (e.g. timber production), carbon sequestration, stand, biodiversity and slope stability in mountainous areas of southern and central Europe (Tinner *et al*., 2013). Dynamic simulations of future vegetation responses to climatic change that consider the past ecology of *A. alba* confirm the high potential of the species under global-warming conditions at local scales [e.g. Swiss Plateau, Ticino (Bugmann *et al*., 2014; Henne *et al*., 2015)]. However, such simulations are currently lacking at the continental scale.

The significant difference between the past and present realized climatic niche and the absence of assessments of *A. alba* potential at a continental scale make it impossible to thoroughly assess how the species may perform in Europe under global warming. Such information is particularly important because forest management measures increasingly include the substitution of the most valuable drought-sensitive European key species *Picea abies* by more drought-tolerant exotic conifer species [(Bolte *et al*., 2009; Temperli *et al*., 2012; Hanewinkel *et al*., 2013); e.g. *Pseutotsuga menziesii*] that have the potential to become invasive and profoundly alter future European forest ecosystems.

Projections of future and past species ranges depend not only on a correct assessment of the climatic niches, but they are also sensitive to past and projected changes in climate. How the climate will evolve on the regional-to-continental scale is determined by several factors (Hawkins & Sutton, 2011). For example, future emissions of carbon and other radiative agents depend on current and future political decisions and other socio-economic developments (Moss *et al*., 2010). Therefore, scenarios are used to describe different plausible future developments and anthropogenic emission pathways. Earth System Models consistently simulate increasing concentrations of greenhouse gases, radiative forcing, a warming trend over Europe, and higher precipitation in northern Europe and less in southern Europe, but the exact magnitudes and patterns of anthropogenically forced changes vary across different models for a given scenario (Stocker *et al*., 2013b). Unforced, natural variability, that is internal to the partly chaotic climate system, is particularly relevant on local to continental spatial scales and on seasonal to decadal time scales (Hawkins & Sutton, 2011). One approach to assess the influence of this internal climate variability is to run ensemble simulations where the same model is repeatedly driven with the same forcing, but for slightly different initial conditions (Deser *et al*., 2012). While multimodel ensemble simulations are standard for the industrial period and the 21st century (Stocker *et al*., 2013b) and in reach for the last millennium (Jungclaus *et al*., 2010), climate simulations for the more distant past are traditionally restricted to particular periods and to single model realizations, given the large CPU and storage requirements of comprehensive Earth System Models (ESMs). Transient runs with an ESM over the last glacial termination [18–11 cal ka BP (thousand years before present)] and the Holocene (11–0 cal ka BP) have only recently become available (Liu *et al*., 2009, 2014).

Here, we use the LPX-Bern dynamic global vegetation model (LPX) to explore the climatic niche of *Abies alba* in Europe under past, present and projected future conditions. To assess its forest-forming potential and thus its realized niche, we simulate its abundance in the vegetation under competition with seven important tree species and the generic LPX plant functional types (PFTs). We rely on the results from previous palaeoecological studies that demonstrate *A. alba* has the potential to grow under warm climatic conditions (Tinner *et al*., 2013; Di Pasquale *et al*., 2014; Cunill *et al*., 2015) and set, as an alternative to other model studies, the bioclimatic limit for the establishment of *A. alba* to a

warm temperature in LPX, while keeping other model parameters and formulations unchanged from previous dynamic global vegetation model studies. The distribution and abundance of *A. alba* is simulated transiently from the Last Glacial Maximum to present, which allows a validation of the model with palaeoecological reconstructions and present-day observations. Specifically, we qualitatively compare the spatiotemporal pattern of the distribution of *A. alba* as simulated by the model with the pattern reconstructed from pollen and macrofossil data for the past 21 000 years, the modern distribution (EUFORGEN, 2009), the modern potential distribution of the species (according to previous correlative simulations by Tinner *et al*., 2013), and ancillary information such as the occurrence of relict tree stands. We use observation-based gridded climate fields to hindcast species distributions in the 20th century and output from a very recent simulation with the Community Earth System Model (CESM) for the past 21 000 years (Liu *et al*., 2009, 2014). For 21st-century simulations, we consider the uncertainty in projected temperature and precipitation arising from uncertainties in anthropogenic emission, climate response uncertainties, and internal, unforced climate variability. This is achieved by forcing LPX with climate output from ensemble simulations with different comprehensive, state-of-the-art Earth System Models (Stocker *et al*., 2013a) and for the representative concentration pathways RCP2.6 (van Vuuren *et al*., 2011) and RCP8.5 (Riahi *et al*., 2011). RCP2.6 is an ambitious, stringent emission mitigation scenario where carbon emissions are phased out over the 21st century. RCP8.5 is a high-emission business-as-usual scenario. The two pathways roughly span the current scenario range in terms of anthropogenic carbon emissions, radiative forcing, and climate outcomes (Van Vuuren *et al*., 2008).

Material and methods

LPX-Bern dynamic global vegetation model

The Land surface Processes and eXchanges model, LPX-Bern model version 1.2 (hereafter LPX) (Spahni *et al*., 2013; Stocker *et al*., 2013a, 2014a,b), is based on the Lund–Potsdam–Jena (LPJ) dynamic global vegetation model (Sitch *et al*., 2003) and has been used in earlier studies to explore carbon, methane, nitrous oxide, vegetation dynamics, and climate feedbacks (Joos *et al*., 2001; Gerber *et al*., 2004; Spahni *et al*., 2011; Zürcher *et al*., 2013). LPX combines process-based, large-scale representations of terrestrial vegetation dynamics, the dynamics of terrestrial carbon and nitrogen stocks and fluxes, and land–atmosphere exchanges of water, carbon dioxide, methane, and nitrous oxide in a modular framework. The model is cost-efficient enough to perform simulations over many thousands of years on the global scale, while complex enough to simulate the distribution of vegetation reasonably well (Smith *et al*., 2001).

LPX simulates the distribution of plant functional types (PFTs) based on bioclimatic limits for plant growth and regeneration, and plant-specific parameters that govern plant competition for light, water (Sitch *et al*., 2003), and nitrogen (Xu-Ri & Prentice, 2008; Xu-Ri *et al*., 2012). PFTs account, in a very broad sense, for the variety of structure and functions among different plants. So-called generic PFTs represent different classes of plants such as boreal, temperate, or tropical evergreen trees, while 'species' are PFTs with parameters assigned to represent an individual plant species. To simulate the performance and development of *A. alba*, this species and seven other ecologically important European trees and shrubs, *Fagus sylvatica, Picea abies, Quercus ilex, Quercus robur, Betula pendula, Corylus avellana,* and *Tilia cordata* were implemented into LPX (Hickler *et al*., 2012), together with the nine existing generic PFTs (tropical broad-leaved evergreen trees, tropical broad-leaved raingreen trees, temperate needle-leaved evergreen trees, temperate broad-leaved evergreen trees, temperate broad-leaved summer green trees, boreal needle-leaved evergreen trees, boreal broadleaved summer green trees, C3 grasses/forbs, and C4 grasses). The additional species are not only competitors of *A. alba,* but also of paramount importance for European vegetation. The original PFTs were retained in our simulations to account for competition from other plants (e.g. *Acer, Alnus, Ulmus, Pinus, Fraxinus, Olea*, and C-4 and C-3 grasses). This procedure reduces the likelihood of overestimating the competitive ability of species and thus the amplitude of their realized niches. The same equations and relationships as used for the corresponding generic PFT are applied for the species (Sitch *et al*., 2003; Gerten *et al*., 2004; Xu-Ri & Prentice, 2008; Spahni *et al*., 2013), although with differences in PFT-specific parameter values.

Physiological, morphological, phenological, bioclimatic, and fire-response attributes describe the generic or species PFTs (Table S2), which represent groups of average individual trees or grass. The bioclimatic limits (Table S2) determine the ability of a PFT to survive and/or regenerate under a particular climate. At the end of each year, the vegetation density is updated based on establishment and mortality of each PFT (Sitch *et al*., 2003). Tree mortality is the result of light competition, low growth efficiency, a negative annual carbon balance, heat stress, or when bioclimatic limits of a PFT are exceeded for an extended time period (Sitch *et al*., 2003). For this study, we implemented and tested the mortality parameterization of Hickler *et al*. (2012) in LPX, which additionally considers different shade-tolerance classes. However, for the standard simulations, we use the original parameterization by Sitch *et al*. (2003) which is PFT independent. Fire fluxes are calculated on the basis of litter moisture content, a fuel load threshold, and PFT-specific fire resistances. Dispersal processes are not explicitly modelled, and an individual PFT can invade new regions if its bioclimatic limits and competition with other PFTs allow establishment.

Seven carbon and nitrogen pools per generic or species PFT represent leaves, sapwood, heartwood, fine roots,

aboveground leaf litter, aboveground woody litter, and belowground litter. Separate soil organic carbon and nitrogen pools receive input from litter of all PFTs. Photosynthesis is modelled using an updated form of the Farquhar scheme and an empirical convective boundary layer parameterization to couple the carbon and water cycle. Net primary productivity is downregulated if N-demand exceeds N-availability from the inorganic soil nitrogen pools, which are subject to leakage and gaseous losses.

Most of the parameters governing species dynamics are set to be identical to those of the corresponding generic PFT (see Table S2). Exceptions are the parameters governing tree height and crown area, fire resistance, and sapwood-to-heartwood turnover, where species-specific values proposed for the LPJ-GUESS model (see Table S1.1 and S1.2 in Hickler *et al*., 2012) are used (Table S2). The parameters governing allocation are set such that tree species, other than *Corylus,* grow potentially larger than the generic PFTs. For example, maximum crown area is set to 27.3 m^2 for the generic PFTs, to 15 m^2 for *Corylus,* and to 40 m^2 for the other species. In other words, these species have the potential to assimilate more carbon per individual than the generic tree PFTs. The parameter governing the fraction of root in the upper (z_1) and lower soil layer and thus access to water is set to shallow rooting (z_1 = 0.8) for *Abies, Fagus, Picea, Betula,* and *Tillia,* to relative deep rooting for *Quercus ilex* (0.5), and to intermediate values for *Quercus robur* and *Corylus,* while a shallow-rooting value (0.7–0.9) is assigned to the generic tree PFTs. The sapwood-to-heartwood conversion rate is set to slow rates [1/(20 years)] for the generic tree PFTs and the shade-tolerant species *Abies, Fagus,* and *Picea,* to intermediate rates for *Quercus* and *Tilia*, and to fast rates for the shade-intolerant species *Betula* and *Corylus*. The value defining fire resistance is set relatively high for *Quercus ilex,* intermediate for *Quercus robur*, and low/normal for the other tree species and the generic boreal and temperate trees. Further, the parameters defining the optimal range and upper limit for photosynthesis for *Abies alba* were refined following the literature summary of Ellenberg (2009). Overall, these parameters are such that the shade-tolerant species tend to dominate over the corresponding generic tree PFT under suitable climate.

Like all dynamic vegetation models, LPX includes many empirical model parameters, and uncertainties in these parameters, in addition to structural uncertainties, may affect the model outcome. For the current study, the most critical model parameters are the bioclimatic limits that describe whether a plant functional type or species can potentially grow under given climatic conditions (Sitch *et al*., 2003; Hickler *et al*., 2012), while uncertainties in other model parameters may appear less critical. In this sense, the most decisive PFT-specific parameters delineating the range of a species or PFT are the bioclimatic limits. A PFT or species cannot survive or establish if these limits are exceeded in the climatological mean. As bioclimatic limits, we use variables that are linked to known physiological mechanisms: minimum winter temperature for survival (*T*c,min), minimum requirement for yearly sum of temperatures above 5 °C (growing degree days; GDD5), and maximum winter temperatures for establishment (Hickler *et al*., 2012). Bioclimatic limits are adopted following Hickler *et al*. (2012), except for the maximum coldest-month temperature for the establishment of *A. alba*. The bioclimatic limits were obtained by combining modern species distribution data and modern climatological data (Sykes *et al*., 1996; Hickler *et al*., 2012). The maximum coldest-month temperature for the establishment of *A. alba* was adjusted to allow *A. alba* to grow in warm areas, as evidenced by cryptic lowland stands in the Mediterranean [e.g. (Pedrotti Cortini, 1967)] and pollen- and macrofossil-based Holocene and Eemian vegetational reconstructions (Tinner *et al*., 2013; Di Pasquale *et al*., 2014) and in agreement with physiological evidence (Boncaldo *et al*., 2010). It is this single parameter, $T_{c,max}$, the maximum winter temperature for establishment, that co-determines whether *A. alba* is allowed to establish in the model under warm winter conditions or not; establishment is only permitted if the minimum monthly temperature is colder than $T_{c,max}$. To this end, we provide results for two contrasting cases where $T_{c,max}$ for *A. alba* is set to a nonlimiting value (technically $T_{c,max}$ is set to 22 °C) and to a value (−2 °C; as in Hickler *et al*., 2012) limiting establishment in regions with warm winters. The nonlimiting case permits *A. alba* to grow in southern Europe in line with relict forest stands and pollen and macrofossil data, whereas *A. alba* does not grow in southern Europe in the limiting case. The model and model parameters of the other generic and species PFTs are used as in earlier work and were not specifically adjusted or tuned for this study.

We present results in terms of foliar projective cover (FPC) or total area coverage. FPC is the fraction of the area within a grid cell that is covered by the considered species or PFT, and total coverage in units of m^2 results from the product of FPC and grid cell area. The sum of FPC for all tree PFTs varies between 0% (bare ground; desert) and 95% (fully vegetated forests), while a fraction of 5% is reserved for grass PFTs or bare ground. In Europe, total FPC for trees is typically 95% (fully vegetated forests). The FPC of an individual species and its total coverage is sensitive to the number of competitor species implemented in the model, and absolute values of FPC and coverage should be interpreted with caution.

Input data and experimental setup

The model simulations in this study were calculated for a 'European domain', here defined as 10°W–42°E, 34°–70°N, with a resolution of 1° by 1° Lat/Lon. Thus, the domain includes parts of northern Africa and western Asia (Fig. 1). The LPX model was run in offline mode and monthly temperature, and precipitation and cloud cover fields as well as atmospheric CO_2, solar insolation, and nitrogen deposition are prescribed. A first spin-up phase under initial conditions extended over 1000 years. Then, soil carbon pool sizes were calculated analytically from annual litter inputs and annual mean decomposition rates, and the spin-up continued for another 500 years. This procedure ensures that slowly overturning soil carbon and nitrogen pools are equilibrated for the LGM and pre-industrial period, respectively (Joos *et al*., 2001).

We ran LPX simulations for three periods, the Last Glacial Maximum (LGM; 22 cal. kyr BP) through 1990 CE, the 20th century, and the 21st century. In a first sensitivity test, the

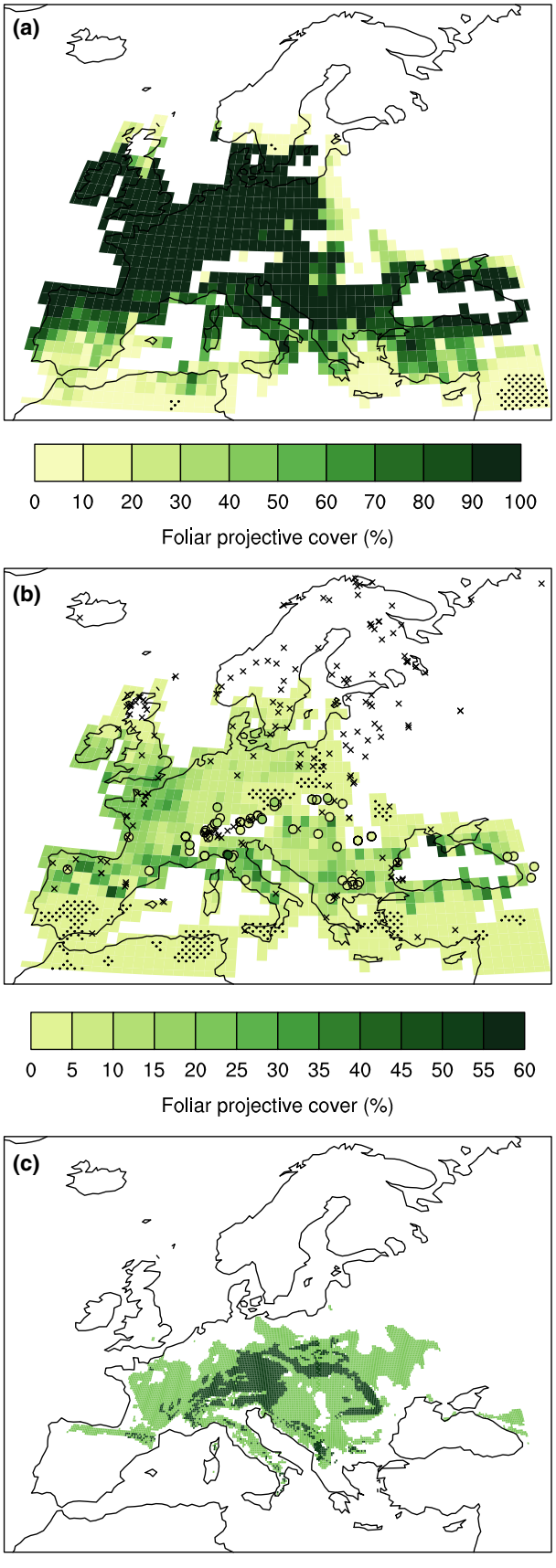

Fig. 1 Modern distribution of *Abies alba*. LPX-Bern dynamic vegetation model simulation of (a) fundamental niche and (b) realized distribution or niche of *Abies alba* in the European model domain for current conditions. Pollen data are used for model evaluation, and values (symbols) are percentages of terrestrial pollen sum; circles represent values above 1%, crosses below 1%. Model results (shading) are for foliar projective cover (FPC) averaged for 1996–2006 CE, and black stippling indicates FPC values between 0 and 1%. The fundamental niche is from a model set-up without competing plant functional types or species. (c) Observation-based modern distribution of *Abies alba* from EUFORGEN (dark shading) and the climatic niche projected for an equilibrium stage with climate (light shading) according to Tinner *et al.* (2013).

distribution of *A. alba* was simulated without competitors during the historical period and a corresponding spin-up. This simulation allowed us to assess the fundamental niche of the species, that is without human impact, competition, or dispersal limitations, with the distribution dependant only on the ecophysiological and climatic limits of the species. The comparison with simulations including competitor species reveals how much competition reduces the abundance of *A. alba*. For the historical run over the 20th century, LPX was forced by the CRU TS 3.21 (Jones & Harris, 2013) observational climate data. The future simulations start at the end of the historical run and were forced by climate anomalies from five CMIP5 models (HadGEM2-ES, MPI-ESM-LR, IPSL-CM5A, MIROC-ESM, CCSM4) as in a previous study (Stocker *et al.*, 2013a). These models cover a wide range of uncertainty with respect to model climate sensitivity and polar amplification. Each model provided the required climate variables for the Representative Concentration Pathways RCP2.6 and RCP8.5 (Riahi *et al.*, 2011; van Vuuren *et al.*, 2011). Other input data, for example global nitrogen deposition and atmospheric CO_2, were prescribed as in Stocker *et al.* (2013a). The simulation starting at the Last Glacial Maximum (LGM) and running until 1990 CE was forced with climate anomalies from the TraCE-21ka CCSM3 model output (Liu *et al.*, 2009) superimposed on the CRU data, orbital variations of solar insolation (Berger, 1977), ice core CO_2 data (Joos & Spahni, 2008), and preindustrial nitrogen deposition. Anthropogenic land use and human-induced fires are not considered. The palaeo and last-century simulations start from an equilibrium state after spin-up.

Pollen data

Pollen data from several sites were extracted from the Alpine Pollen Database of University of Bern (ALPADABA) and the European Pollen Database (EPD) and used for comparison with modelling results. We selected representative European sites (Table S1) with good to excellent temporal precision and resolution. The chronologies follow the latest insights: they either follow the original publications or later publications, or are refinements made in the databases, and are based on radiocarbon dates in a few cases supplemented by unproblematic pollen-stratigraphic dates such as the start of the

Holocene. The number of sites decreases with increasing time, given that only a few sites reach the LGM. Pollen percentages were calculated following standard procedures, excluding spores and pollen of aquatic and wetland plants. We amalgamated adjacent pollen samples to form 500 cal. year steps to show trends. Choosing 500 year time intervals has the advantages of reducing noise in the pollen data and minimizing the risk of amalgamating samples that do not belong to the same period. Taxonomic determination beyond the genus is not possible with *Abies* pollen, while macrofossils (e.g. needles) allow species determination, so that the range history can be reconstructed (Terhürne-Berson *et al.*, 2004). The palaeodata are used to evaluate the model outcome. They are not used for model tuning or to constrain model parameters.

Results

Modern distribution of Abies alba

In a first step, the distribution was simulated without any competitors to assess the modern fundamental niche of the species (Fig. 1a). In the absence of other species, dispersal limitations, and human influence, *A. alba* is simulated to grow very well in western, central, and southern Europe and the Black Sea region.

LPX simulations with seven competitor species and nine generic PFTs allow us to estimate the modern potential range of *A. alba* in the absence of human management impacts (Fig. 1b). The current distribution of *A. alba* (EUFORGEN, 2009) (Fig. 1c), potential range estimated from the present realized climatic niche (Tinner *et al.*, 2013), and pollen-inferred mid-Holocene range (Figs 2 and 3a) all fall within the distribution simulated by LPX with present climate (1996–2006 CE) (Fig. 1b). However, the LPX-simulated distribution of *A. alba* covers a larger area, especially in north-western Europe, specifically the British Isles. The misrepresentation of *A. alba* in the British Isles and north-western Europe likely reflects model deficiencies such as the consideration of few bioclimatic limits, the absence of simulated grazing, an underestimation of dispersal limits, and a simplified representation of edaphic factors. LPX also simulates *A. alba* in areas where it does not grow today in southern Spain, Sicily, Greece, northern Africa, and the Black Sea region. However, closely related *Abies* species (e.g. *A. pinsapo, A. nebrodensis, A. cephalonica, A. numidica, A. cilicica, A. nordmanniana, A. bornmuelleriana*), which are not explicitly represented in the model, grow in these areas (Aussenac, 2002; Liepelt *et al.*, 2009),

Spatiotemporal evolution of Abies alba over the past 21 000 years

The pollen data permit us to confront model results for *A. alba* with observational evidence for radically different climatic conditions and for the transgression from cold glacial to warm interglacial conditions and over the rapid, decadal-scale cold–warm–cold–warm swings associated with the Bølling–Allerød (14.6–12.5 cal ka BP) warm and Younger Dryas (12.5–11.6 cal ka BP) cold period (Figs 2 and 3). Overall, pollen data and model results yield a consistent picture of an expanding abundance and a northward and eastward range expansion of *A. alba* over the deglaciation. The most noticeable mismatch regards the LGM and the early Late Glacial prior to ca. 14.0 cal. ka BP, for which the

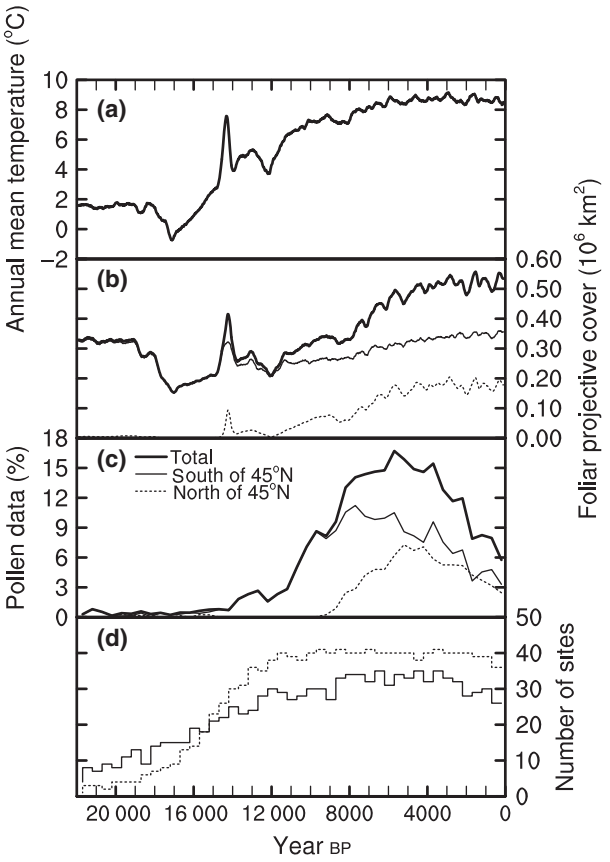

Fig. 2 Deglacial expansion of *Abies alba* abundance for the European domain as inferred from pollen data and simulated with LPX-Bern. (a) Annual mean surface air temperature (200 year running average) as estimated from temperature anomalies simulated by the Community Earth System Model in the TraCE-21ka experiment and observations. (b) Simulated foliar projective cover (FPC) of *A. alba* over the European domain (solid line), south of 45°N (thin solid) and north of 45°N (dashed) as simulated by LPX-Bern forced by TraCE-21ka climate anomalies (200 year running average). (c) Pollen percentages for *Abies* for the European domain (solid), south of 45°N (thin solid) and north of 45°N (dashed). The basis for calculation of pollen percentages includes terrestrial trees, shrubs, and herbs (see methods). (d) Number of pollen sites south (thin solid) and north (dashed) of 45°N.

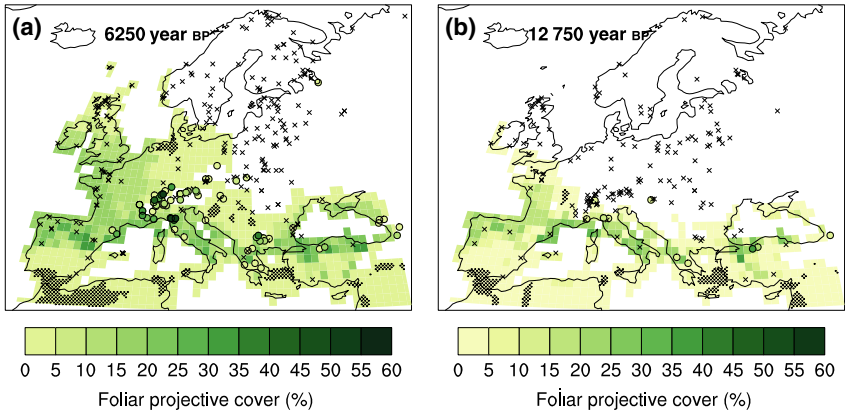

Fig. 3 Distribution of *Abies alba* in the European domain for (a) the mid-Holocene (6.5 to 6 cal ka BP) and (b) during the Bølling–Allerød (13.0–12.5 cal ka BP) periods as inferred from pollen data and simulated with LPX-Bern. Pollen values (symbols) are *Abies* percentages of terrestrial pollen sum; circles represent values above 1%, crosses below 1%. Model results (shading) are for foliar projective cover (FPC), and black stippling indicates FPC values between 0 and 1%.

palaeo data exclude any relevance of the species (Fig. 2b, c). In contrast, LPX simulates frequent abundance of *A. alba* in southern Europe (south of 45°N) during the LGM (21–18 cal ka BP), followed by a decrease during the early part of the glacial termination (18–14.6 cal ka BP). Similarly, the expansion of *A. alba* north of 45°N occurs several millennia earlier in the model than in the pollen data. It is not known whether this data-model mismatch is the result of deficiencies in the climate forcing data (e.g. too warm and/or humid conditions) or of deficiencies in the LPX model only. In any case, model deficiencies identified for modern conditions such as widespread abundance in the British Isles, the Black Sea region, Sicily, north Africa, and Iberia, which may partly relate to vicariant species of *Abies* filling the climatic niche of *A. alba*, are also present in the palaeo simulation (Fig. 3) and likely led to biases in spatially aggregated coverage.

Our combined modelling and pollen results suggest that the Bølling–Allerød interstadial (14.6–12.5 cal ka BP) initiated the expansion of *A. alba* in southern Europe. The simulated expansion in southern Europe at the onset of Bølling–Allerød (~14.6 cal ka BP) is in reasonable agreement with the palaeoecological evidence (Fig. 2b, c). Subsequently, the species declined in both the simulations and the pollen data during the Younger Dryas cold period (12.5–11.6 cal. ka BP). Rapid climate warming at the onset of the Holocene (ca. 11.6 cal. ka BP) led to an expansion of *A. alba* that continued to the mid-Holocene in both the simulations and the palaeo records.

By the end of the Bølling–Allerød, LPX simulates in agreement with pollen data, the almost complete absence of *A. alba* north of the Alps and in eastern Europe (Fig. 3b). We note that there are a few sites with small pollen percentages (<1%) of *Abies*. Pollen data suggest abundant *Abies* at the Ligurian Coast and Côte d'Azur, in Greece and in northern Turkey; in all these regions, high foliar projective cover (FPC) is simulated by LPX (Fig. 3b). Again, the model simulates the occurrence of *A. alba* in France and the Iberian Peninsula in contrast to palaeoecological evidence. *A. alba* reached its peak expansion in the pollen record by the mid-Holocene (Fig. 2c). Comparison of the spatially resolved pollen and model results for the end of the Bølling–Allerød (Fig. 3b) and the mid-Holocene (Fig. 3a) reveal a consistent northward and eastward expansion of *A. alba* between the two periods. Overall, the model does well in simulating the distribution in most areas of Europe, while in southern Spain, Sicily, western Asia, and northern Africa, other species of *Abies* fill the climatic niche of *A. alba* (Lang, 1994; Liepelt *et al.*, 2009). The pollen data points in the Alps are not very well captured, probably due to the coarse model resolution.

Abies pollen percentages decrease after 6.0 cal. ka BP, but *Abies* FPC stays fairly constant or even increases in the simulation. The number of sites providing pollen data north and south of 45°N increases until about 12.0 cal. ka BP and then remains quite constant until 1990 CE (Fig. 2d). The decline of *Abies* in pollen percentages in Fig. 2c cannot therefore be linked to a smaller number of sites analysed, but may instead have been caused by early human influence in Europe. Land-use pressure, excessive anthropogenic fire, and browsing disturbance caused substantial declines of *A. alba* coverage over the last 5000 years, especially in the Mediterranean region, where anthropogenic pressure was strong enough to cause local extinctions (Colombaroli *et al.*, 2007; Henne *et al.*, 2013; Tinner *et al.*, 2013).

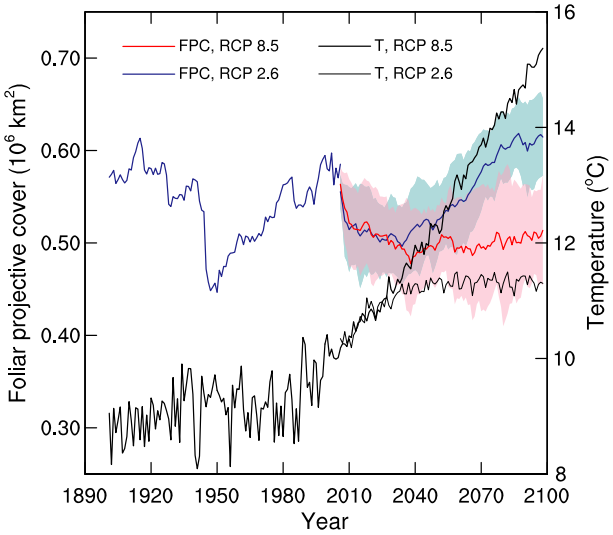

Fig. 4 Temporal evolution of foliar projective cover of *Abies alba* integrated over the European domain for the industrial period (blue) and the 21st century for the high-emission RCP8.5 (red) and the stringent emission mitigation (blue) RCP2.6 pathways. Shadings represent ±1SD around the multimodel ensemble means (solid). Black lines show observation-based and ensemble mean annual mean surface air temperature for RCP8.5 (solid) and RCP2.6 (thin solid) averaged over the European domain.

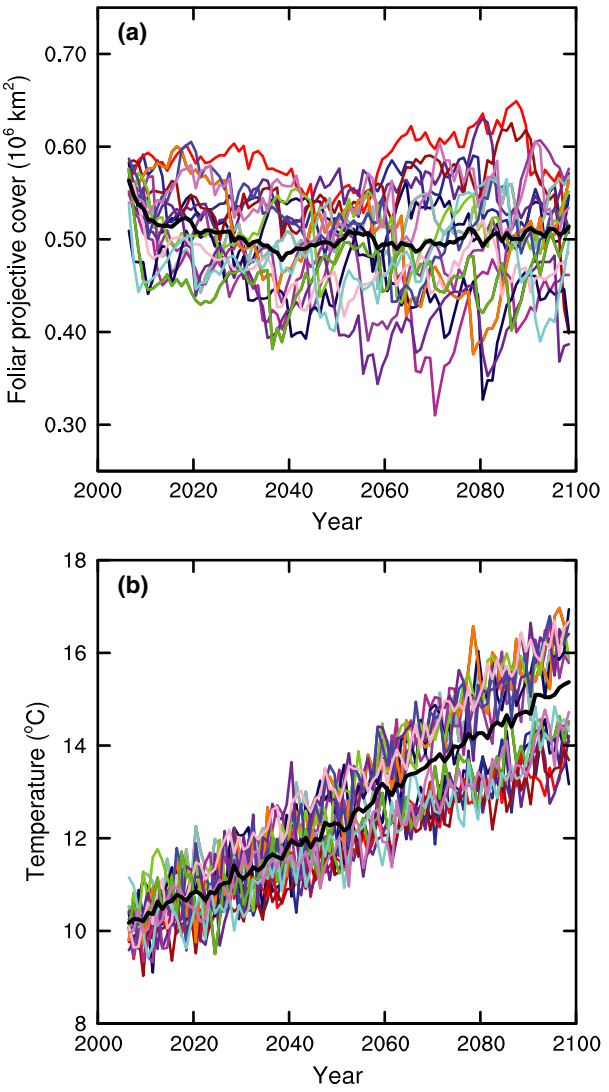

Fig. 5 Spread in model projections for (a) foliar projective cover of *Abies alba* and (b) annual mean surface air temperature for the European domain. Climate results are from an ensemble of twenty simulations with five different climate models and used to force the LPX-Bern dynamic vegetation model. Results are for RCP8.5, and ensemble means are given by thick lines. The MPI-ESM-LR and the CCSM4 climate models project a lower-than-average surface warming, whereas the IPSL-CM5A-LR, MIROC-ESM, and the HadGEM models project a higher-than-average warming.

Industrial period and projections over the 21st century

The simulations over the industrial period and the 21st century suggest that the FPC by *A. alba* integrated over the European domain remains fairly constant (Figs 4 and 5) for the range of scenarios. However, there are shifts in the spatial distribution for the high-emission RCP8.5 scenario with a decline of *A. alba* in southern Europe and expansion in parts of eastern Europe (Fig. 6). Total modelled coverage by *A. alba* in the European domain varies roughly within 45 and 60 million km^2 over the industrial period. There is a relatively sharp decline on the order of 20% in FPC by *A. alba* in the 1940s and a slow recovery thereafter. The decline is linked to a decrease in precipitation by up to 50% in Italy, Spain, central Europe, and around the Black Sea between 1939 and 1948 CE. This caused the top soil layer to become drier and therefore less suitable for the growth of *A. alba* in the model. There is also variability observed in tree ring growth for *A. alba* in Europe (Büntgen *et al.*, 2014). However, this variability is not directly comparable to our model results as we do not take into account the influence of changes in forest management or sulphur deposition.

Ensemble mean and individual projections show that integrated FPC of *A. alba* varies roughly within the 20th century range for both RCPs (Figs 4 and 5). On average, integrated coverage of *A. alba* slightly decreases at the beginning of the 21st century. Integrated coverage remains stable under RCP8.5 and slightly expands under RCP2.6 until 2100 CE. Ensemble mean surface temperature increases by around 5 °C in RCP8.5 and by 1 °C in RCP2.6 over the 21st century. Individual simulations with LPX as forced by climate anomalies from individual climate ensemble simulations show a considerable spread in integrated coverage (Fig. 5a). This is linked to differences in the space–time evolution

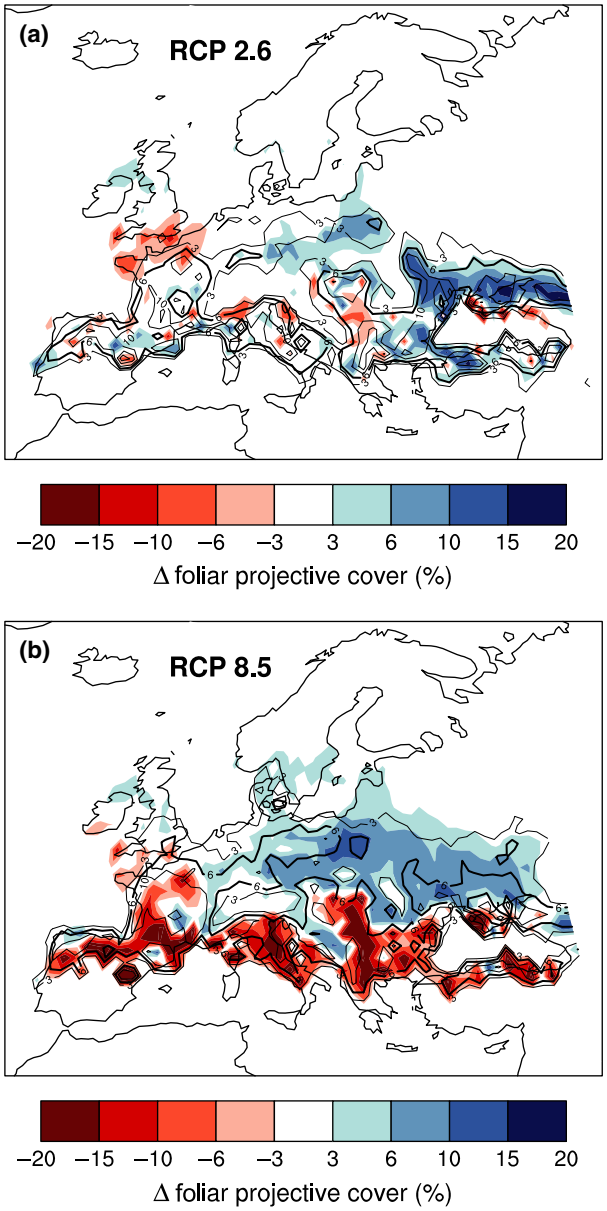

Fig. 6 Projected 21st-century changes in *Abies alba* abundance for (a) the stringent emission mitigation pathway RCP2.6 and (b) the high-emission pathway RCP8.5. Shadings represent ensemble mean changes (2099–2006) in foliar projective cover of *A. alba* and contour lines one standard deviation around the ensemble mean. Contour spacing follows the colour scale and the 6% contour line is in bold.

of precipitation and temperature in the multimodel ensemble as illustrated by the differences in projected mean surface air temperature between individual ensemble members (Fig. 5b).

In the projected changes in the spatial distribution of *A. alba* over the 21st century and for the stringent emission mitigation pathway RCP2.6 (Fig. 6a), FPC hardly changes in the current range of *A. alba* (Fig. 1b), except for a decline in parts of northern France and southern England and an increase in coverage around the Black Sea. On the other hand, *A. alba* significantly expands its range in parts of eastern Europe and large areas north of the Black Sea (e.g., Poland, Belarus, Ukraine). The climatic changes under the stringent emission mitigation pathway RCP2.6 are small enough to avoid any massive dieback of *A. alba* at the warm limit of its potential range in southern Europe and northern Turkey, but large enough to enable expansion in eastern Europe in our model.

Under the high-emission RCP8.5 (Fig. 6b), there are large and widespread reductions in potential *A. alba* coverage in southern Europe (e.g. northern Spain, France, Italy, Greece, Macedonia, Serbia, Bulgaria) and northern Turkey and a northward and eastward expansion in eastern Europe that is even larger than under RCP2.6. *A. alba* generally grows in areas where annual precipitation does not fall below 700–800 mm per year (Tinner *et al.*, 2013). The dry and hot conditions projected for RCP8.5 are responsible for the decrease in FPC of *A. alba* in southern Europe. The projected changes in FPC exceed the one standard deviation range of our ensemble simulations and are thus robust across the range of temperature and precipitation forcings. However, in some warm areas where projections of FPC decrease, such as all of Italy, *A. alba* had already strongly declined during the late Holocene (Figs 1b, 2c and 3a), probably in response to land use. In other potential range areas such as northern Iberia outside the Pyrenees, the species presumably never played a prominent role (Figs 1 and 3).

Sensitivity simulations

The above results could be sensitive to the choice of model parameters and formulations. To this end, we investigated the sensitivity to differences in the parameterization of tree mortality and to prescribed bioclimatic limits. A PFT-dependent mortality parameterization (Hickler *et al.*, 2012) was implemented into LPX and compared to the PFT-independent mortality parameterization applied as a standard. While absolute values of FPC of *A. alba* are sensitive to the mortality parameterization, the geographical range and changes in the geographical range of *A. alba* are generally not sensitive, and the main findings presented above are robust for the two schemes. The PFT-dependent mortality parameterization caused the FPC of *A. alba* to increase especially in northern Europe and the UK, leading to a larger mismatch between model results and observational evidence than for the standard setup. We tested the bioclimatic limit for the establishment of new *A. alba* saplings. This is specified as the maximum

coldest-month temperature ($T_{c,max}$) and establishment is suppressed if monthly mean temperatures do not, on climatological average, fall below this limit. Hickler *et al.* (2012) applied a limit of −2 °C, much lower than the standard limit of 22 °C used in this study for *A. alba*, that is the limit adopted from the generic PFT representing temperate needle-leaved evergreen trees (Sitch *et al.*, 2003). In a sensitivity simulation, $T_{c,max}$ for *A. alba* was set to −2 °C, which dramatically reduced the geographical range of *A. alba* (Fig. 7a), especially in southern and central Europe. This is in clear contrast with observational evidence, and the distribution of *A. alba* with $T_{c,max}$ of −2 °C is neither compatible with the pollen data (Fig. 7a) nor reality [*A. alba* stands are known to grow under competition at $T_{c,max}$>5 °C, (Tinner *et al.*, 2013)]. Projected changes under RCP8.5 are very different for the two alternative temperature limits (Figs 6b and 7b). Generally, simulated changes in FPC are much smaller for the case with $T_{c,max}$ of −2 °C than for our standard model set-up. These results demonstrate the importance of considering both palaeoecological and modern observational evidence for the quantification of climate change impacts in terms of future species shifts.

Discussion

In this study, we assessed past and projected distribution of *A. alba* in Europe. A goal is to provide information that is potentially useful for the planning of emission mitigation and adaption measures to limit the impacts of global warming. We combined palaeoecological evidence using pollen data and modern observations with results from the LPX dynamic vegetation model as forced by the best available quantification of past and future climate change from comprehensive Earth System Models to project stability of *A. alba* in central Europe under global warming.

Uncertainties in our approach arise from uncertainties in vegetation model formulations, disturbance regimes, climate input, and palaeo data. LPX-Bern constrains the potential geographical range of trees with a limited number of bioclimatic parameters, and here on a grid with a resolution of 1° × 1°. Finer-scale geographical features, differences in daily temperature ranges, or occurrence of extreme events and disturbances by animal grazing and management are not explicitly considered. On the other hand, the model is validated against a broad set of observational evidence (Sitch *et al.*, 2003; Steinacher *et al.*, 2013). LPX is also able to hindcast the spatial pattern and the magnitude of change in intrinsic water-use efficiency as reconstructed from stable carbon isotope data from a European-scale tree ring network (Saurer *et al.*, 2014), lending support to model formulations. For the projections, we quantified uncertainties related to climate input data by employing results from a multimodel ensemble and for two bounding climate scenarios. For

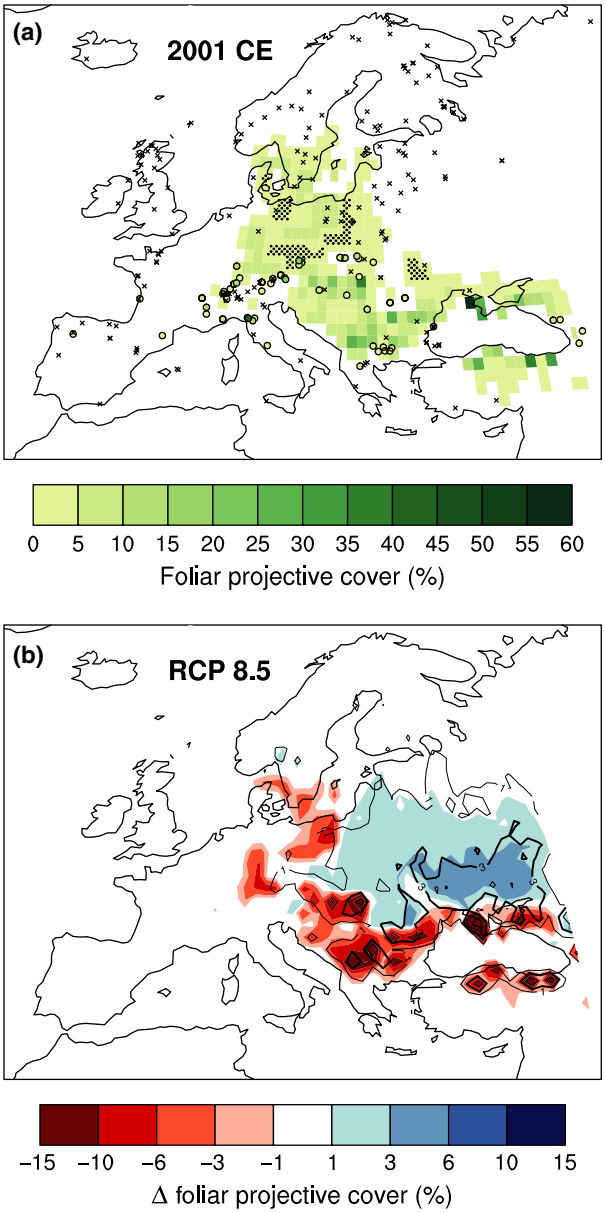

Fig. 7 An alternative bioclimatic limit for the establishment of *Abies alba*. Simulated (a) modern distribution and (b) projected 21st-century change (2099–2006) for a model setup where maximum coldest-month temperature ($T_{c,max}$) for establishment is set to −2 °C instead of 22 °C as in the standard set-up. This suppresses *A. alba* establishment in all regions where monthly mean temperatures do not fall below −2 °C. Projections are for RCP8.5 and shadings show ensemble mean changes and contour lines one standard deviation around the ensemble mean. Contour spacing follows the colour scale, and the 3% contour line is in bold.

the past, we relied on output from a single simulation over the past 21 000 years with the Community Earth System Model. Similar studies using different vegetation models and potentially updated climate information would be desirable to further confirm the robustness of our results. Uncertainties in palaeo data arise inter alia from the scarcity of suitable pollen and macrofossil records in many regions and from the potentially limited representativeness of existing records.

Simulations from the LGM to the 20th century nicely reproduce the occurrence of *A. alba* in southern Europe and its expansion towards northern Europe as reconstructed from the palaeo data. This implies that the model captures vegetation responses to climatic changes such as those associated with the Younger Dryas cooling or the onset of the Holocene. These results provide support for the projected changes and suggest that LPX is suited for climate change response analyses at the European scale.

Under present climate, the LPX-Bern model generally simulates *A. alba* within its range and where pollen data show its abundance (Fig. 1). However, differences in the simulated potential distribution and the realized distribution today are large in north-western Europe and the Black Sea region (Fig. 1). Geographical barriers (e.g. North Sea), dispersal capacity, distance from refugia, vicariant species (e.g. *A. nordmanniana* in the Black Sea region), and other biotic and abiotic effects [e.g. disturbance, soils, pathogens; (Giesecke *et al*., 2007; Tinner *et al*., 2013)] may partially explain this discrepancy. However, the presence of large areas of suitable climate where *A. alba* does not grow today supports the conclusion that nonclimatic factors, in particular human impacts, are critical constraints (Tinner *et al*., 2013; Di Pasquale *et al*., 2014).

Although *A. alba* is a strong competitor when disturbance is infrequent, several characteristics limit regeneration success as the frequency and intensity of disturbance increase. In contrast to important competitors (e.g. *Fagus, Quercus*), *A. alba* does not resprout following fire or cutting and has a long generation time, producing seeds only after 60–70 years. *A. alba* is also a favoured browse species, and grazing by wild and domestic ungulates limits regeneration. LPX does not consider human disturbances that likely suppressed *A. alba* in southern Europe. Indeed, the model simulates present forest growth in southern Europe (Fig. 1), where the species has become locally extinct during the late Holocene most likely in response to excessive human impact [e.g. Mediterranean coast, lowlands of central and southern Italy (Colombaroli *et al*., 2007; Bellini *et al*., 2009; Henne *et al*., 2013; Di Pasquale *et al*., 2014)]. This finding is in excellent agreement with local-scale dynamic vegetation models that suggest without human disturbance, *A. alba* would still form forests in the southern European coastlands, where moisture availability is sufficient to support its growth (Henne *et al*., 2013).

Our results provide support that *A. alba* does not require cold winters to establish in contrast to earlier studies. The relevant bioclimatic limit, the maximum winter temperature for establishment, $T_{c,max}$, is set for *A. alba* to the same limit (22 °C) and used for the generic PFT representing temperate needle-leaved evergreen trees. This permits establishment also in regions with warm winter climate as evidenced by the pollen record and remaining refugia or relict stands in southern Europe. Much lower thresholds are implemented in various process-based models [e.g. −3.0 °C: (Bugmann & Solomon, 2000; Cailleret *et al*., 2014); −2.0 °C: (Hickler *et al*., 2012)], which limit *A. alba* populations in regions with mild winters such as north-west Europe, where today it does not form forests. However, a low $T_{c,max}$ also eliminates *A. alba* in regions where it was widespread during the mid-Holocene (Tinner *et al*., 2013; Di Pasquale *et al*., 2014) (Figs 3 and 7) and is not supported by physiological studies. For example, *A. alba* is propagated following cold stratification at 4 °C (Boncaldo *et al*., 2010) and occurs and regenerates spontaneously in cryptic forest patches close to Pisa at $T_{c,max}$ 7–8 °C (Pedrotti Cortini, 1967). Thus, dynamic and species distribution models that derive ecophysiological constraints from today's distributions alone risk severely underestimating the present and future potential, especially for late-successional trees that are sensitive to human impacts. By considering palaeoecological data that demonstrate the former abundance of *A. abies* in regions of southern Europe with mild winter temperatures, our study avoids this complication.

For the 21st century, our results suggest that *A. alba* will expand to the north-east in Europe, in the absence of excessive human land-use pressure, in response to climate warming both for the mitigation pathway RCP2.6 and even more pronouncedly for the high-emission RCP8.5. The warming alleviates restrictions by bioclimatic limits, and *A. alba* is able to expand to areas that were previously too cold. Despite its potential expansion to north-eastern Europe, *A. alba* growth is still maintained in its present realized niche under 21st-century warming, whereas its potential range is projected to shrink in southern Europe and northern Turkey under RCP8.5.

Our new dynamic modelling results project stability of *A. alba* in southern Europe under the moderate warming scenario of RCP2.6, but substantial losses under the pronounced warming scenario RCP8.5 (Fig. 6). Such mass extinctions of populations will most

likely not occur, given that today's southern European *A. alba* stands or forests are, with the exception of a very few cryptic warmth-loving stands [e.g. (Pedrotti Cortini, 1967)], confined to moist and cool habitats at intermediate to high altitudes (>800–1000 m a.s.l.; (Mayer, 1984; Rovelli, 1995), a bioclimatic situation comparable to that of silver fir forests in central Europe.

The projections over the 21st century show that *A. alba* is able to maintain its modern range in central Europe despite strong competition from the other species and the generic PFTs included in the model. Bioclimatic analyses of *A. alba* show that if compared with other important forest-forming species such as *Quercus robur*, *Fagus sylvatica*, or *Picea abies*, the species has a far more limited filling of its potential range (Tinner *et al*., 2013) and thus of its (present) realized climatic niche (Pearson & Dawson, 2003). Disequilibrium with climate, for example through browsing pressure, impedes a thorough assessment of future species responses with species distribution (SDM) or bioclimatic envelope models, and this explains why our findings contradict the SDM study by Maiorano *et al*. (2013) that suggests a reduction of climate suitability for *A. alba* in response to even moderate warming during the next decades. However, our projected stability of *A. alba* in central Europe is in excellent agreement with results from dynamic landscape vegetation models at local scales (ca. 5 km^2) (Henne *et al*., 2013; Bugmann *et al*., 2014). Evidence of beneficial effects of climate warming on *A. alba* includes tree ring series showing unprecedented growth of *A. alba* in central Europe during the past decades (Büntgen *et al*., 2014; Gazol *et al*., 2015).

In conclusion, available evidence suggests that *Abies alba* is able to grow under projected climate change in central Europe and the mountain areas of southern Europe (>800–1000 m a.s.l.), where it is abundant today. This implies that the species will not need to adapt under global warming conditions, neither by migration nor by genetic adaptation strategies. Thus, *A. Alba* may provide important ecosystem services, complementing those by other species. *A. Alba* may ensure stand and slope stability and avalanche protection, thereby protecting traffic, tourism, and settlement infrastructure. It may provide surface cooling during hot days through transpiration and thereby limit heat stress. *A. alba* may provide a high potential for maintaining productivity and for protecting carbon stocks in European forests during the next centuries.

Acknowledgements

We thank B. Otto-Bliesner and Z. Liu for providing TraCE-21ka CCSM3 model output. This study is supported by the Swiss National Science Foundation (SNF) through the grant to the Division of Climate and Environmental Physics (200020-14174) and the Sinergia Project iTREE (CRSII3_136295). SNF project contributions (200021_134616, PP002-114886) to the division of Palaeoecology are also gratefully acknowledged.

References

Anderson NJ, Bugmann H, Dearing JA, Gaillard M-J (2006) Linking palaeoenvironmental data and models to understand the past and to predict the future. *Trends in Ecology & Evolution*, **21**, 696–704.

Aussenac G (2002) Ecology and ecophysiology of circum-Mediterranean firs in the context of climate change. *Annals of Forest Science*, **59**, 823–832.

Bellini C, Mariotti-Lippi M, Montanari C (2009) The Holocene landscape history of the NW Italian coasts. *The Holocene*, **19**, 1161–1172.

Berger A (1977) Long-term variations of earths orbital elements. *Celestial Mechanics*, **15**, 53–74.

Bolte A, Ammer C, Löf M *et al*. (2009) Adaptive forest management in central Europe: climate change impacts, strategies and integrative concept. *Scandinavian Journal of Forest Research*, **24**, 473–482.

Boncaldo E, Bruno G, Sicoli G, Tommasi F, Mastropasqua L (2010) Germinability and fungal occurrence in seeds of *Abies alba* Mill. Populations in southern Italy. *Plant Biosystems*, **144**, 740–745.

Bugmann HKM, Solomon AM (2000) Explaining forest composition and biomass across multiple biogeographical regions. *Ecological Applications*, **10**, 95–114.

Bugmann H, Brang P, Elkin C *et al*. (2014) Climate change impacts on tree species, forest properties, and ecosystem services. In: *CH-2014 Impacts, Toward Quantitative Scenarios of Climate Change Impacts in Switzerland* (eds Raible CC, Strassman KM), pp. 79–89. Oeschger Centre for Climate Change Research, Bern.

Büntgen U, Tegel W, Kaplan JO *et al*. (2014) Placing unprecedented recent fir growth in a European-wide and Holocene-long context. *Frontiers in Ecology and the Environment*, **12**, 100–106.

Cailleret M, Heurich M, Bugmann H (2014) Reduction in browsing intensity may not compensate climate change effects on tree species composition in the Bavarian Forest National Park. *Forest Ecology and Management*, **328**, 179–192.

Cheaib A, Badeau V, Boe J *et al*. (2012) Climate change impacts on tree ranges: model intercomparison facilitates understanding and quantification of uncertainty. *Ecology Letters*, **15**, 533–544.

Colombaroli D, Marchetto A, Tinner W (2007) Long-term interactions between Mediterranean climate, vegetation and fire regime at Lago di Massaciuccoli (Tuscany, Italy). *Journal of Ecology*, **95**, 755–770.

Cunill R, Métailié J-P, Galop D, Poublanc S, de Munnik N (2015) Palaeoecological study of Pyrenean lowland fir forests: Exploring mid–late Holocene history of *Abies alba* in Montbrun (Ariège, France). *Quaternary International*, **366**, 37–50.

Deser C, Knutti R, Solomon S, Phillips AS (2012) Communication of the role of natural variability in future North American climate. *Nature Climate Change*, **2**, 775–779.

Di Pasquale G, Allevato E, Cocchiararo A, Moser D, Pacciarelli M, Saracino A (2014) Late Holocene persistence of *Abies alba* in low-mid altitude deciduous forests of central and southern Italy: new perspectives from charcoal data. *Journal of Vegetation Science*, **25**, 1299–1310.

Ellenberg HH (2009) *Vegetation Ecology of Central Europe*. Cambridge University Press, Cambridge.

Ellenberg H, Leuschner C (2010) *Vegetation Mitteleuropas mit den Alpen*. Verlag Eugen Ulmer, Stuttgar.

EUFORGEN (2009) *European Forest Genetic Resources Programme*. Biodiversity International, Maccarese Rome, Italy, www.euforgen.org.

García-Valdés R, Zavala MA, Araújo MB, Purves DW (2013) Chasing a moving target: projecting climate change-induced shifts in non-equilibrial tree species distributions. *Journal of Ecology*, **101**, 441–453.

Gazol A, Camarero JJ, Gutiérrez E *et al*. (2015) Distinct effects of climate warming on populations of silver fir (*Abies alba*) across Europe. *Journal of Biogeography*, **42**, 1150–1162.

Gerber S, Joos F, Prentice IC (2004) Sensitivity of a dynamic global vegetation model to climate and atmospheric CO_2. *Global Change Biology*, **10**, 1223–1239.

Gerten D, Schaphoff S, Haberlandt U, Lucht W, Sitch S (2004) Terrestrial vegetation and water balance - hydrological evaluation of a dynamic global vegetation model. *Journal of Hydrology*, **286**, 249–270.

Giesecke T, Hickler T, Kunkel T, Sykes MT, Bradshaw RHW (2007) Towards an understanding of the Holocene distribution of *Fagus sylvatica* L. *Journal of Biogeography*, **34**, 118–131.

Hanewinkel M, Cullmann DA, Schelhaas M-J, Nabuurs G-J, Zimmermann NE (2013) Climate change may cause severe loss in the economic value of European forest land. *Nature Climate Change*, **3**, 203–207.

Hawkins E, Sutton R (2011) The potential to narrow uncertainty in projections of regional precipitation change. *Climate Dynamics*, **37**, 407–418.

Henne PD, Elkin CM, Reineking B, Bugmann H, Tinner W (2011) Did soil development limit spruce (*Picea abies*) expansion in the Central Alps during the Holocene? Testing a palaeobotanical hypothesis with a dynamic landscape model. *Journal of Biogeography*, **38**, 933–949.

Henne P, Elkin C, Colombaroli D, Samartin S, Bugmann H, Heiri O, Tinner W (2013) Impacts of changing climate and land use on vegetation dynamics in a Mediterranean ecosystem: insights from paleoecology and dynamic modeling. *Landscape Ecology*, **28**, 819–833.

Henne P, Elkin C, Franke J *et al.* (2015) Reviving extinct Mediterranean forest communities may improve ecosystem potential in a warmer future. *Frontiers in Ecology and the Environment*, **13**, 356–362.

Hickler T, Vohland K, Feehan J *et al.* (2012) Projecting the future distribution of European potential natural vegetation zones with a generalized, tree species-based dynamic vegetation model. *Global Ecology and Biogeography*, **21**, 50–63.

IPCC (2014) Summary for policy makers (WG II). In: *Climate Change 2014: Impacts, Adaptation and Vulnerability. Part A: Global and Sectoral Aspects. Contribution of Working Group II to the Fifth Assessment Report of the Intergovernmental Panel on Climate Change* (eds Field CB, Barros VR, Dokken DJ, Mach KJ, Mastrandrea MD, Bilir TE, Chatterjee M, Ebi KL, Estrada YO, Genova RC, Girma B, Kissel ES, Levy AN, Maccracken S, Mastrandrea PR, White LL), pp. 1–32. Cambridge University Press, Cambridge, UK and New York, NY, USA.

Jones P, Harris I (2013) *CRU TS3.21: Climatic Research Unit (CRU) Time-Series (TS) Version 3.21 of High Resolution Gridded Data of Month-by-Month Variation in Climate (January 1901 – December 2012)*. NCAS British Atmospheric Data Centre. Available at: http://badc.nerc.ac.uk/view/-badc.nerc.ac.uk__ATOM__ACTIVITY_0c08abfc-f2d5-11e2-a948-00163e251233 (accessed 24 September 2014).

Joos F, Spahni R (2008) Rates of change in natural and anthropogenic radiative forcing over the past 20,000 years. *Proceedings of the National Academy of Sciences of the United States of America*, **105**, 1425–1430.

Joos F, Prentice IC, Sitch S *et al.* (2001) Global warming feedbacks on terrestrial carbon uptake under the Intergovernmental Panel on Climate Change (IPCC) emission scenarios. *Global Biogeochemical Cycles*, **15**, 891–908.

Jungclaus JH, Lorenz SJ, Timmreck C *et al.* (2010) Climate and carbon-cycle variability over the last millennium. *Climate of the Past*, **6**, 723–737.

Küster H (1997) The role of farming in the postglacial expansion of beech and hornbeam in the oak woodlands of central Europe. *The Holocene*, **7**, 239–242.

Lang G (1994) *Quartäre Vegetationsgeschichte Europas. Methoden und Ergebnisse*. Gustav Fischer Verlag Jena, Stuttgart, New York.

Liepelt S, Cheddadi R, de Beaulieu J-L *et al.* (2009) Postglacial range expansion and its genetic imprints in *Abies alba* (Mill.) — A synthesis from palaeobotanic and genetic data. *Review of Palaeobotany and Palynology*, **153**, 139–149.

Liu Z, Otto-Bliesner BL, He F *et al.* (2009) Transient simulation of last deglaciation with a new mechanism for bolling-allerod warming. *Science*, **325**, 310–314.

Liu Z, Zhu J, Rosenthal Y *et al.* (2014) The Holocene temperature conundrum. *Proceedings of the National Academy of Sciences of the United States of America*, **111**, E3501–E3505.

Maiorano L, Cheddadi R, Zimmermann NE *et al.* (2013) Building the niche through time: using 13,000 years of data to predict the effects of climate change on three tree species in Europe. *Global Ecology and Biogeography*, **22**, 302–317.

Markgraf V (1970) Palaeohistory of the Spruce in Switzerland. *Nature*, **228**, 249–251.

Mayer H (1984) *Waldbau auf Soziologisch-Ökologischer Grundlage*. Gustav Fischer Verlag, Stuttgart, Germany.

Meier ES, Lischke H, Schmatz DR, Zimmermann NE (2012) Climate, competition and connectivity affect future migration and ranges of European trees. *Global Ecology and Biogeography*, **21**, 164–178.

Moss RH, Edmonds JA, Hibbard KA *et al.* (2010) The next generation of scenarios for climate change research and assessment. *Nature*, **463**, 747–756.

Overpeck J, Whitlock C, Huntley B (2003) Terrestrial biosphere dynamics in the climate system: past and future. In: *Paleoclimate, Global Change and the Future* (eds Alverson KD, Bradley RS, Pedersen TF), pp. 81–111. Springer, Berlin.

Pearson RG, Dawson TP (2003) Predicting the impacts of climate change on the distribution of species: are bioclimate envelope models useful? *Global Ecology and Biogeography*, **12**, 361–371.

Pedrotti Cortini C (1967) L'abetina di varramista (Pisa). *Webbia*, **22**, 39–65.

Poulter B, Pederson N, Liu H *et al.* (2013) Recent trends in Inner Asian forest dynamics to temperature and precipitation indicate high sensitivity to climate change. *Agricultural and Forest Meteorology*, **178–179**, 31–45.

Ralska-Jasiewiczowa M, Nalepka D, Goslar T (2003) Some problems of forest transformation at the transition to the oligocratic/Homo sapiens phase of the Holocene interglacial in northern lowlands of central Europe. *Vegetation History and Archaeobotany*, **12**, 233–247.

Riahi K, Rao S, Krey V *et al.* (2011) RCP 8.5—A scenario of comparatively high greenhouse gas emissions. *Climatic Change*, **109**, 33–57.

Rovelli E (1995) La distribuzione dell'abete (*Abies alba* Mill.) sull'Appennino. *Monti e Boschi*, **6**, 5–13.

Saurer M, Spahni R, Frank DC *et al.* (2014) Spatial variability and temporal trends in water-use efficiency of European forests. *Global Change Biology*, **20**, 3700–3712.

Schröter D, Cramer W, Leemans R *et al.* (2005) Ecosystem service supply and vulnerability to global change in Europe. *Science*, **310**, 1333–1337.

Schwörer C, Henne PD, Tinner W (2014) A model-data comparison of Holocene timberline changes in the Swiss Alps reveals past and future drivers of mountain forest dynamics. *Global Change Biology*, **20**, 1512–1526.

Schwörer C, Colombaroli D, Kaltenrieder P, Rey F, Tinner W (2015) Early human impact (5000–3000 BC) affects mountain forest dynamics in the Alps. *Journal of Ecology*, **103**, 281–295.

Sitch S, Smith B, Prentice IC *et al.* (2003) Evaluation of ecosystem dynamics, plant geography and terrestrial carbon cycling in the LPJ dynamic global vegetation model. *Global Change Biology*, **9**, 161–185.

Smith B, Prentice IC, Sykes MT (2001) Representation of vegetation dynamics in the modelling of terrestrial ecosystems: comparing two contrasting approaches within European climate space. *Global Ecology and Biogeography*, **10**, 621–637.

Spahni R, Wania R, Neef L *et al.* (2011) Constraining global methane emissions and uptake by ecosystems. *Biogeosciences*, **8**, 1643–1665.

Spahni R, Joos F, Stocker BD, Steinacher M, Yu ZC (2013) Transient simulations of the carbon and nitrogen dynamics in northern peatlands: from the Last Glacial Maximum to the 21st century. *Climate of the Past*, **9**, 1287–1308.

Steinacher M, Joos F, Stocker TF (2013) Allowable carbon emissions lowered by multiple climate targets. *Nature*, **499**, 197–201.

Stocker BD, Roth R, Joos F *et al.* (2013a) Multiple greenhouse-gas feedbacks from the land biosphere under future climate change scenarios. *Nature Climate Change*, **3**, 666–672.

Stocker TF, Dahe Q, Plattner G-K *et al.* (2013b) Technical summary. In: *Climate Change 2013: The Physical Science Basis. Contribution of Working Group I to the Fifth Assessment Report of the Intergovernmental Panel on Climate Change* (eds Stocker TF, Qin D, Plattner G-K, Tignor M, Allen SK, Boschung J, Nauels A, Xia Y, Bex V, Midgley PM), pp. 33–115. Cambridge University Press, Cambridge, UK and New York, NY, USA.

Stocker BD, Feissli F, Strassmann KM, Spahni R, Joos F (2014a) Past and future carbon fluxes from land use change, shifting cultivation and wood harvest. *Tellus Series B*, **66**, 1–15.

Stocker BD, Spahni R, Joos F (2014b) DYPTOP: a cost-efficient TOPMODEL implementation to simulate sub-grid spatio-temporal dynamics of global wetlands and peatlands. *Geoscientific Model Development*, **7**, 3089–3110.

Sykes MT, Prentice IC, Cramer W (1996) A bioclimatic model for the potential distributions of north european tree species under present and future climates. *Journal of Biogeography*, **23**, 203–233.

Temperli C, Bugmann H, Elkin C (2012) Adaptive management for competing forest goods and services under climate change. *Ecological Applications*, **22**, 2065–2077.

Terhürne-Berson R, Litt T, Cheddadi R (2004) The spread of Abies throughout Europe since the last glacial period: combined macrofossil and pollen data. *Vegetation History and Archaeobotany*, **13**, 257–268.

Thuiller W, Lavorel S, Araújo MB, Sykes MT, Prentice IC (2005) Climate change threats to plant diversity in Europe. *Proceedings of the National Academy of Sciences of the United States of America*, **102**, 8245–8250.

Tinner W, Colombaroli D, Heiri O *et al.* (2013) The past ecology of *Abies alba* provides new perspectives on future responses of silver fir forests to global warming. *Ecological Monographs*, **83**, 419–439.

Van Vuuren DP, Meinshausen M, Plattner G-K *et al.* (2008) Temperature increase of 21st century mitigation scenarios. *Proceedings of the National Academy of Sciences of the United States of America*, **105**, 15258–15262.

van Vuuren D, Stehfest E, den Elzen MJ *et al.* (2011) RCP2.6: exploring the possibility to keep global mean temperature increase below 2°C. *Climatic Change*, **109**, 95–116.

Xu-Ri, Prentice IC (2008) Terrestrial nitrogen cycle simulation with a dynamic global vegetation model. *Global Change Biology*, **14**, 1745–1764.

Xu-Ri, Prentice IC, Spahni R, Niu HS (2012) Modelling terrestrial nitrous oxide emissions and implications for climate feedback. *New Phytologist*, **196**, 472–488.

Zürcher S, Spahni R, Joos F, Steinacher M, Fischer H (2013) Impact of an abrupt cooling event on interglacial methane emissions in northern peatlands. *Biogeosciences*, **10**, 1963–1981.

Supporting Information

Additional Supporting Information may be found in the online version of this article:

Figure S1. Average July precipitation in Europe for 1901–1910 CE (a) and the precipitation anomalies compared to (a) for (b) 12.7 cal. ka BP (July average for 12.95–12.45 cal. ka BP), (c) Mid-Holocene 6.25 cal. ka BP (July average for 6.5–6.0 cal. ka BP), and (d) July average for 2090–2099 CE with RCP8.5. The average July precipitation in Europe for 1995–2005 CE is always subtracted from the respective period. Spatial resolution is 1° × 1°.
Figure S2. Average July temperature in Europe for 1901–1910 CE (a) and the temperature anomalies compared to (a) for (b) 12.7 cal. ka BP (July average for 12.95–12.45 cal. ka BP), (c) Mid-Holocene 6.25 cal. ka BP (July average for 6.5–6.0 cal. ka BP), and (d) July average for 2090–2099 CE with RCP8.5. The average July temperature in Europe for 1995–2005 CE is always subtracted from the respective period. Spatial resolution is 1° × 1°.
Figure S3. Distribution of *Abies alba* and competitor species in Europe in 2001 CE (average for 1996–2006 CE) with spatial resolution of 1° × 1°. (a) *Abies alba*, (b) *Fagus sylvatica*, (c) *Picea abies*, (d) *Quercus ilex*, (e) *Quercus robur*. The black stippling indicates FPC values below 1%.
Figure S4. Distribution of *Abies alba* and competitor species without generic PFTs in Europe in 2006 CE with spatial resolution of 1° × 1°. (a) *Abies alba*, (b) *Fagus sylvatica*, (c) *Picea abies*, (d) *Quercus ilex*, (e) *Quercus robur*. The black stippling indicates FPC values below 1%.
Table S1. Location of pollen data from the European Pollen Database (EPD) and the Alpine Palynological Database (ALPADABA) as used in this study.
Table S2. PFT and species-specific parameters.